Larisa ARESHKINA
United Institute of Informatics Problems, NAS of Belarus, 6 Surganova str., Minsk, 220012, Belarus
e-mail: ola@newman.bas-net.by

VEGETATION IN RECOGNITION OF CHANGES IN EARTH REMOTE SENSING IMAGES

Summary

The method has been developed for recognition of changes, caused by vegetation, using the Earth remote sensing data obtained at different points of time. The method includes automatic calculation of brightness groups in segments of changes for each range in the multizonal image. Also, the problem of the spatial multispectral decomposition is resolved with regard to the areas of changes caused by vegetation, with the automatic selection of the object's components homogeneous in terms of their reflection properties.

1. Introduction

The results of various natural, anthropogenic and technical impacts, affecting the ecosystems, determine the necessity to use the remote sensing data not only to detect the changes in the Earth surface area that is subject to observation, but also to obtain the information about the nature and causes of these changes. Besides the importance of the resulting knowledge about the processes in the ecosystems, this information is important in economic terms, because it can serve as a basis for solving many practical problems, such as prevention and detection of the before-mentioned impacts and evaluation of their consequences.

Now, several approaches are available [1-3] that are capable to reveal the abnormal changes in vegetation, using the satellite imagery time series for several years and the vegetation indices. For example, the NDBI time series difference method is based on calculation of the mean value and the standard deviation (σ) and determination of thresholds for n classes of spectral changes in vegetation.

However, the level of automatic data processing in these methods remains low. Implementation of these approaches includes tedious interactive procedures in which the human operator must participate to solve the decoding problems, and many applications cannot be implemented in real time, especially with the amounts of satellite imagery information growing stably. Therefore, for the modern remote monitoring systems, special attention must be paid to the implementation of fully automatic procedures and algorithms for processing the data received from satellites [4]. These automatic procedures and algorithms provide opportunities to obtain real information that does not depend on personal opinions of any specialists.

Investigations and developments of principles of the selective brightness-based segmentation of changes [5, 6] and spatial spectral decomposition of multispectral ranges in the changes revealed in the objects covered by the satellite observations (within these procedures, the brightness-based groups are recognized in the changes of each spectral range, and the vectors of multispectral reflecting properties of natural objects are calculated) have resulted in development of the algorithm for automatic selection of changes caused by the vegetation.

The important results include elimination of the interactive approach and development of the algorithm for automatic calculation of specified characteristics. Due to the simplicity of calculation, the normalized difference vegetation index (NDVI) was chosen for use in this algorithm; the NDVI is calculated for each satellite imagery time series and quantitatively characterizes the plants biomass development level.

In this work, the remote sensing data from two satellites were used, Landsat ETM + (for July 21, 1999, and June 5, 2000, Minsk Region, Belarus, 28.5 m spatial resolution) and QuickBird (May 15 and July 16, 2007, Brest Region, Belarus, 0.6 m spatial resolution).

2. Modern solutions for the problem of recognition of changes in the satellite monitoring of the Earth surface objects

During the years of development of the Earth remote sensing, many methods were proposed to reveal the changes [7 – 11]. These methods are based on the information about the specific features of the light flux reflection from different components of the underlying surface. It was recognized that the change detection, although being the different in each particular case, complicated and multi-aspect process, involves several most common methods, such as the image differencing, principal component difference and post-classification comparison. The mixture spectral analysis, artificial neural networks, and the GIS and remote sensing data integration have become the most applicable methods for change detection in practical problems.

Unfortunately, there is no universal approach for classification and application of methods that use space technologies to detect the changes on the Earth surface. The one of the first designers of such methods, A. Singh [7], has proposed to classify them in two types, the classification comparison and the pixel-by-pixel comparison. D. Lu et al [8] have described all possible approaches for the change detection and has classified them into seven categories: arithmetic operations, transformation, classification comparison, advanced models, GIS integration, visual analysis and other approaches. The seventh category (the other approaches) includes the change detection methods that are not suitable to be included in any of six other categories and are not still applied for practical purposes. Also, the requirements for image preprocessing necessary to detect the changes were discussed here; however, fully automatic implementation of any appropriate method was not even mentioned. In [9], the method was described, in which the dictionary of deterministic and rank criteria, based on the difference histogram, was used to detect the changes in the object appearance. This approach has provided an opportunity to implement an automatic search for changes in the monitored objects and to develop the solutions for new problems involving the satellite imagery recognition.

Finally, John Richards et al [10] have summarized the change detection methods and have proposed the classification system for them. The classes include the image differencing, the statistical hypothesis method (the method in which the decision-making is based on the experimental data), the forecast modeling, the illumination modeling (polygon filling / object filling), the background modeling etc. However, the authors have not emphasized these methods' application for the remote sensing.

In spite of their variety, all methods using the satellite observations to detect the changes in the monitored objects on the Earth surface are based on the comparison of the information obtained at different points of time. These methods use the information about the specific features of the spectral reflection from various components of the monitored surface. Here, the images obtained earlier at the specified calendar time, or other spatially-coordinated data describing the object, such as digital maps or GIS databases, serve as the sources of information describing the object's current appearance.

The brightness value combinations that provide information about the monitored object make it possible to determine the object's spectral index, also referred to as the vegetation index. Now, about 160 versions of the vegetation index are in use. Each index is used as some function of reflectance values demonstrated by the vegetation and soils [3] observed by the researcher in particular practical conditions. The difference vegetation index is one of the most common methods applied to detect the changes. The index in each pixel is used to construct the image; as a result, the object of interest can be detected, or its condition can be assessed.

Many factors affect the detection results, including the weather conditions, season, the Sun angle, terrain illumination etc; therefore, the satellite imagery preprocessing is necessary to make the changes detectable. The requirements for preprocessing are different, depending on the change detection method applied in a particular case. Now, the radiometric correction algorithms are the most common; these algorithms basically consist of the image regression methods, pseudoinvariant components, dark and light level normalization, histogram normalization, matching, modeling of the satellite signal in the solar spectrum etc.

For many change detection methods, the exact spatial referencing is necessary, or the satellite imagery obtained at different points of time must be matched. The importance of these procedures is obvious, because any displacement relative to the specified coordinates affects the detection results.

3. Automatic detection of changes in the satellite imagery objects resulting from vegetation

The fundamental researches in physiology and biophysics have demonstrated that the most important factors determining the vegetation elements' optical properties, are the pigment and water content in their tissues, and, also, their morphological structure. These factors determine the selectivity of the vegetation elements' optical properties throughout the spectrum [12]. In this respect, when the multizonal images are used to detect the object changes in the applications involving the remote sensing, in many cases, not absolute values but the particular relations between the object brightness values in various spectral ranges are of importance.

When the object's appearance changes, the changes in its component's reflection properties result in replacement of this component, total or partial, within the object area, while the object area always remains constant [5]. It should be noted that the surface materials or elements, that have formed the brightness distribution in the image, disappear partially or fully and are replaced by other elements when the object appearance is changed. To detect these cases on the satellite imagery, the image's difference diagrams are commonly recommended. These diagrams characterize the object changes in a specific way (see Figure 1).

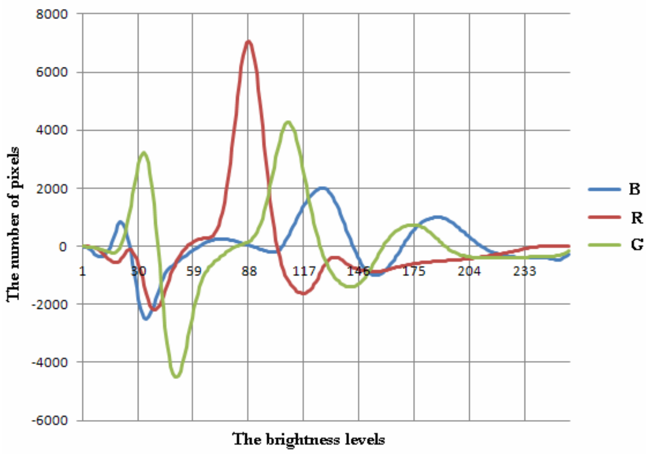

Figure 1. Changes of brightness of non-uniform components resulting in difference between the initial histogram and the changed one in each channel

Figure 1 demonstrates that, along with the positive changes (the term "positive" means the sign) in histograms caused by the emergence of components with their areas having new reflection properties, the negative changes are also possible, caused by the component areas reduction because of their replacement by the new components. This fact serves as a basis for the selective brightness-based segmentation of any changes of the satellite imagery object in each spectral range [6].

Therefore, the development of the algorithm for the automatic analysis of the vegetation-related changes is based on the approach that includes, at the first stage, the selective brightness-based segmentation of changes for each range of the multizonal image. For the initial data used at this stage, see Figure 2.

At the first stage of detection of the vegetation-related changes in the satellite imagery objects the selective brightness-based segmentation is applied for all changes detected in the satellite imagery at different points of time. The algorithm for its implementation shall be as follows [6]:

1) Determine the difference histogram for the satellite imagery object:

$$\Delta H(L) = H(L) - H_0(L), \qquad (1)$$

where $H_0(L)$ is the histogram of the reference image, obtained as a characteristic of the object's "normal" condition, any deviations from which are of interest and shall be considered as the object's appearance changes;

$H(L)$ is the histogram of the current object imagery, intended for the monitoring for possible deviations from the "normal" condition;

L are the brightness values.

a)

b)

c)

d)

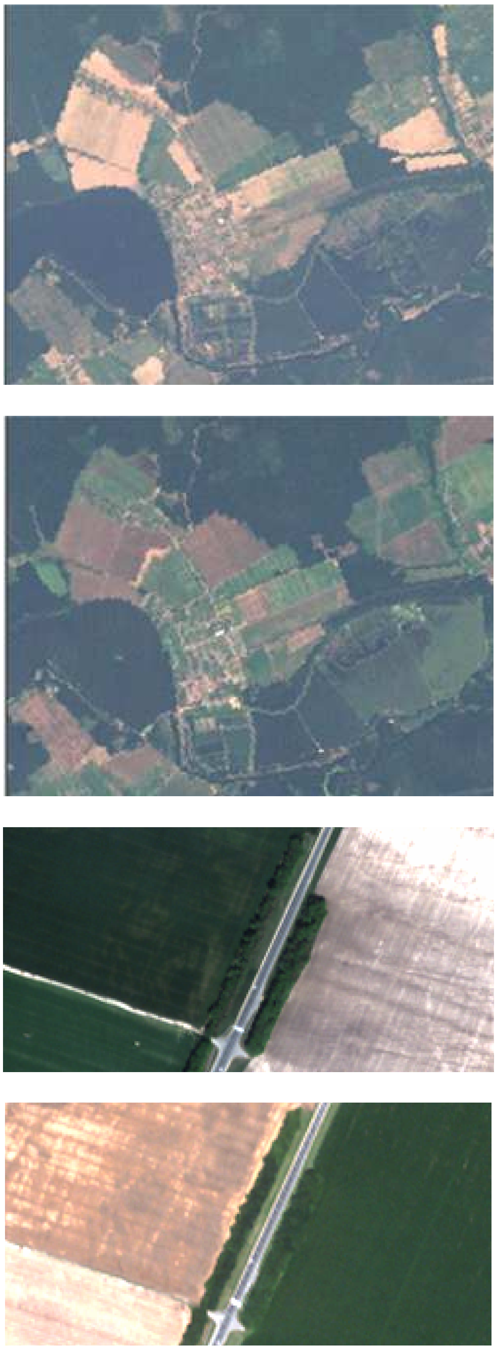

Figure 2. Terrain area images obtained at different points of time: Landsat satellite, June 05, 2000 and July 21, 1999 (a, b) and QuickBird satellite, May 15, 2007 and July 16, 2007 (c, d)

2) Determine the positive brightness change intervals, $L^{+}_{p\min} \div L^{+}_{p\max}$, as the grouping brightness ranges[1], related to the emergence of components that are new in terms of their brightness properties, meeting the condition:

$$\Delta H(L) > 0 \quad , \tag{2}$$

where $\Delta H(L)$ is the difference histogram;

p is the change interval number.

[1] It should be noted that, under real conditions, determination of the groupings interval to the level of pixels, $\Delta H(L)$, includes a separate task intended to overcome the image noise affecting this procedure.

3) Determine the negative brightness change intervals, $L^{-}_{q\min} \div L^{-}_{q\max}$, as the pixel grouping brightness ranges, related to the object's component areas reduction caused by their replacement by the new components meeting the condition:

$$\Delta H(L) \le 0 \quad , \tag{3}$$

where $\Delta H(L)$ is the difference histogram;

p is the number of the interval of positive groupings in the difference histogram.

4) Determine the spatial position of components of the reference image having the brightness values within the range of pth change, as a transition from the brightness-based distribution of pixels in the histogram, $\Delta H(L)$, to the spatial brightness-based distribution of the image, $L_0(x,y)$; finally, the image shall be transformed into binary form, and the result shall be expressed as a set:

$$B_{p0}(x,y) = \begin{cases} 1 & \text{при} \quad L_0(x,y,t_1) \in \left(L_{p\min} \div L_{p\max}\right); \\ 0 & \text{при} \quad L_0(x,y,t_1) \notin \left(L_{p\min} \div L_{p\max}\right), \end{cases} \tag{4}$$

5) Determine the spatial position of components of the image in the current imaging of the object, having the brightness values within the range of pth change, as a similar transition from the brightness-based distribution of pixels in the histogram, $\Delta H(L)$, to the spatial brightness-based distribution; finally, the image shall be transformed into binary form, and the result shall be expressed as a set:

$$B_{p}(x,y) = \begin{cases} 1 & \text{при} \quad L(x,y,t_2) \in \left(L_{p\min} \div L_{p\max}\right); \\ 0 & \text{при} \quad L(x,y,t_2) \notin \left(L_{p\min} \div L_{p\max}\right), \end{cases} \tag{5}$$

6) Determine the spatial position of components of the reference image having the brightness values within the ranges of negative grouping; finally, the image shall be transformed into binary form, and the result shall be expressed as a set:

$$B^{-}_{\Sigma}(x,y) = \begin{cases} 1 & \text{при} \quad L_0(x,y,t_1) \in \left(L_{q\min} \div L_{q\max}\right) \quad \forall q; \\ 0 & \text{при} \quad L_0(x,y,t_1) \notin \left(L_{q\min} \div L_{q\max}\right) \quad \forall q, \end{cases} \tag{6}$$

where q is the number of the interval of negative groupings in the difference histogram.

7) Determine the segments of the spatial position of pth change within the time interval between the imageries, as a difference between the binary sets (4) and (5), consisting of pixels having a unit brightness, where each pixel is characterized by the coordinates of position in the image space:

$$B_{p\Delta}(x,y) = B_p(x,y) \setminus B_{p0}(x,y) \, . \tag{7}$$

8) Partial elimination of geometric correction defects and noise surges within pth brightness interval (these drawbacks are common for the satellite imagery), as an intersection of binary sets, $B_{p\Delta}(x,y)$ and $B^{-}_{\Sigma}(x,y)$:

$$B_{p\Delta}(x,y) = B_{p\Delta}(x,y) \bigcap B^{-}_{\Sigma\, p}(x,y) \tag{8}$$

At the second stage, the problem of the spatial multispectral decomposition of the areas of changes is resolved for each satellite imagery object, affected by the single-spectrum appearance change. Because the objects are characterized by the areas of change, with the surfaces composed of multispectral components, the spatial multispectral decomposition provides an opportunity to find the intersections of selected one-range areas of changes found during the first stage of the selective brightness-based segmentation. These intersections are two-range ($V_{kl}^{RG}(x,y)$, $V_{k0m}^{RB}(x,y)$) and three-range ($V_{klm}^{RGB}(x,y)$) subareas of the components of changes in the object's space; the subareas contain several brightness intervals of the spectral components of channels (*k, l* and *m*). In such a case, the source data are as follows:

– sets of multispectral changes in each range of brightness values, found during the first stage of the selective brightness-based segmentation of the object's changes in all spectral ranges and their combinations:

$$\left(M_1^R, M_2^R, ..., M_{NR}^R; M_1^G, M_2^G, ..., M_{NG}^G; M_1^B, M_2^B, ..., M_{NB}^B\right) \qquad (9)$$

– intervals of brightness of changes in each spectral range:

$$\left(L_{N\min}^{+R} \div L_{N\max}^{+R}\right), \left(L_{N\min}^{+G} \div L_{N\max}^{+G}\right), .., \left(L_{N\min}^{+B} \div L_{N\max}^{+B}\right) \qquad (10)$$

The number of selected current multispectral changes depends on whether the intersections of the one-range areas of changes are true. For this purpose, several intersection images are thinned by elimination of empty sets from them:

$V_l^{RG} = \varnothing$, $V_k^{RB} = \varnothing$, $V_m^{RGB} = \varnothing$, where $l = \overline{0, NRG}$, $k = \overline{0, NRB}$, $m = \overline{0, NRGB}$.

During the third stage, the vegetation-related changes are selected. To assess the vegetation condition, the NDVI [13] scale is used (see Figure 3).

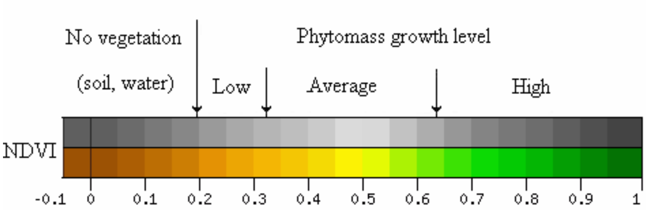

Figure 3. NDVI and corresponding vegetation types in summer vegetation period

For the flowchart of the algorithm used to detect and analyze the vegetation-related changes of the object's appearance, see Figure 4.

To calculate the set of derivative images of changes, $L_N^R(x,y)$ and $L_N^{IR}(x,y)$, for R and IR ranges, the N th image of two-range ($V_{kl}^{RG}(x,y)$, $V_{k0m}^{RB}(x,y)$) and three-range subareas of the components of changes, $V_{klm}^{RGB}(x,y)$, is multiplied, element-by-element, by the reference image of the R and IR ranges. During this procedure, together with the multispectral subareas of the components of changes, the time series of the images in the IR range is stored in the database. For the selected segment of changes in the brightness interval, the spectral index is calculated as follows:

$$V_I(x,y) = ((L_N^{IR}(x,y) - L_N^R(x,y)) / ((L_N^{IR}(x,y) + L_N^R(x,y)) . \qquad (11)$$

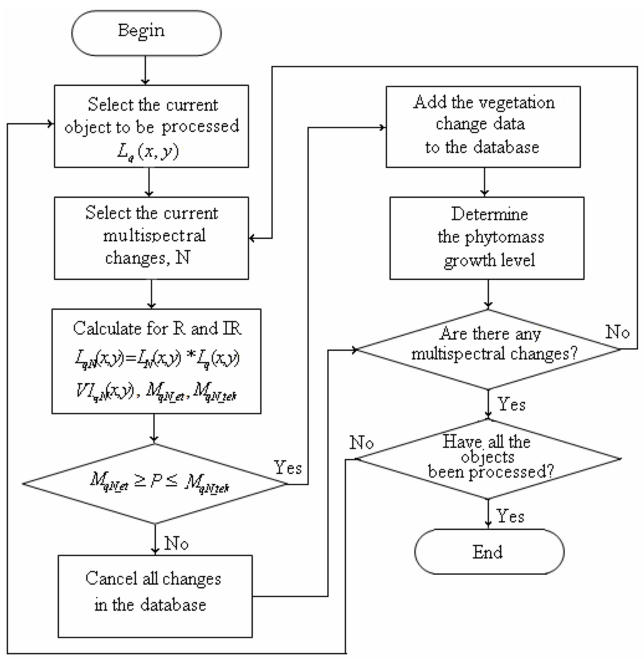

Figure 4. Algorithm for detection of the vegetation-related changes

Because the reflection factor of the uniform surface area is characterized by the probabilistic distribution which is specific for this area, the number of non-uniform components, comprising the imagery surface, is the same as the number of the specific reflection distributions, with their mean values and root-mean-square spreads characterizing this surface. It should be noted that, as a rule, the distribution of both non-uniform and uniform components of the Earth surface area, included in the image, is non-uniform within this area. To analyze the vegetation changes between the time series of the satellite imagery, the representativeness threshold is set, $M_э \geq 0{,}5 \leq M$, based on calculation of the mean value, $M = \frac{1}{J}\sum_{j=1}^{J} V$; the threshold describes the vector of changes of the object for the particular spatial location and characterizes the mean level of the phytomass growth for the purpose of assessment of the vegetation living condition or absence.

4. Experimental application results

The relation between the spectral ranges, determined at the second stage of the algorithm, provides an opportunity to analyze the subareas of the components of changes in the object's space, containing several combinations of the spectral components together.

For the results of calculations for the spectral components of the index images of the spatially-distributed brightness-based multispectral segments of changes in the satellite imagery obtained at different points of time, see Figures 5-8.

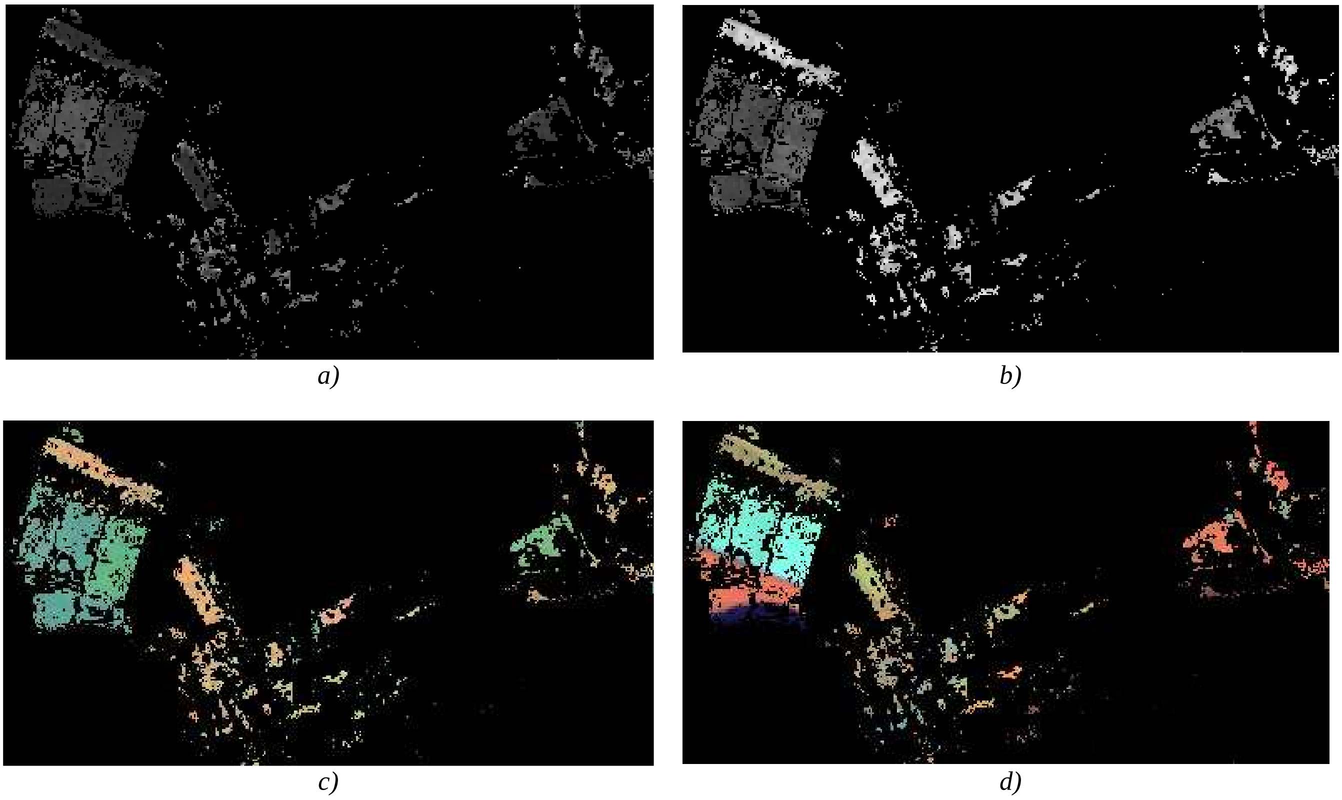

Figure 5. NDVI calculation results for multispectral segments of RB-changes, (5a, 5b) index gray-scale segments of the images obtained from Landsat, June 05, 2000 and July 21, 1999, (5c, 5d) pseudocolor index images

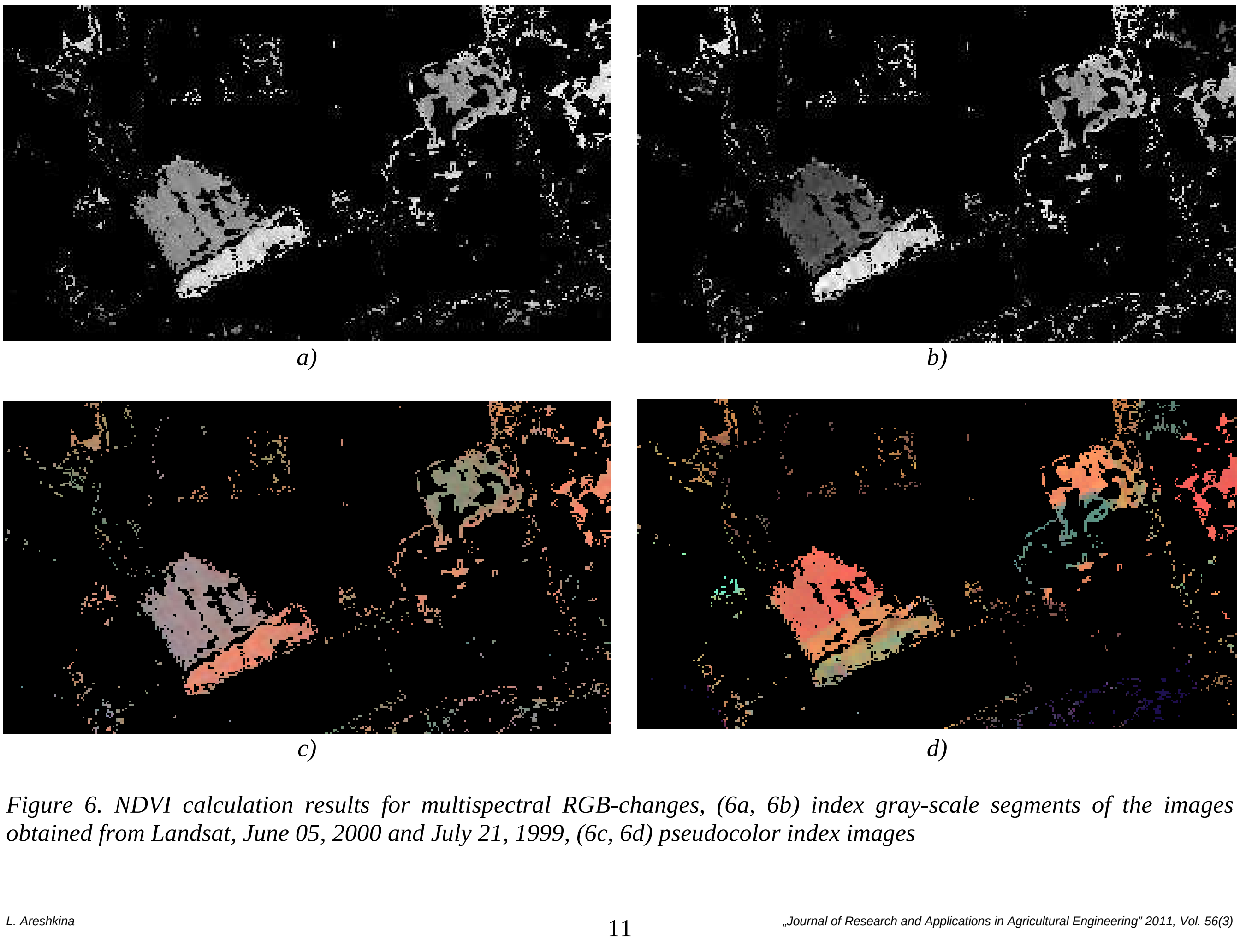

Figure 6. NDVI calculation results for multispectral RGB-changes, (6a, 6b) index gray-scale segments of the images obtained from Landsat, June 05, 2000 and July 21, 1999, (6c, 6d) pseudocolor index images

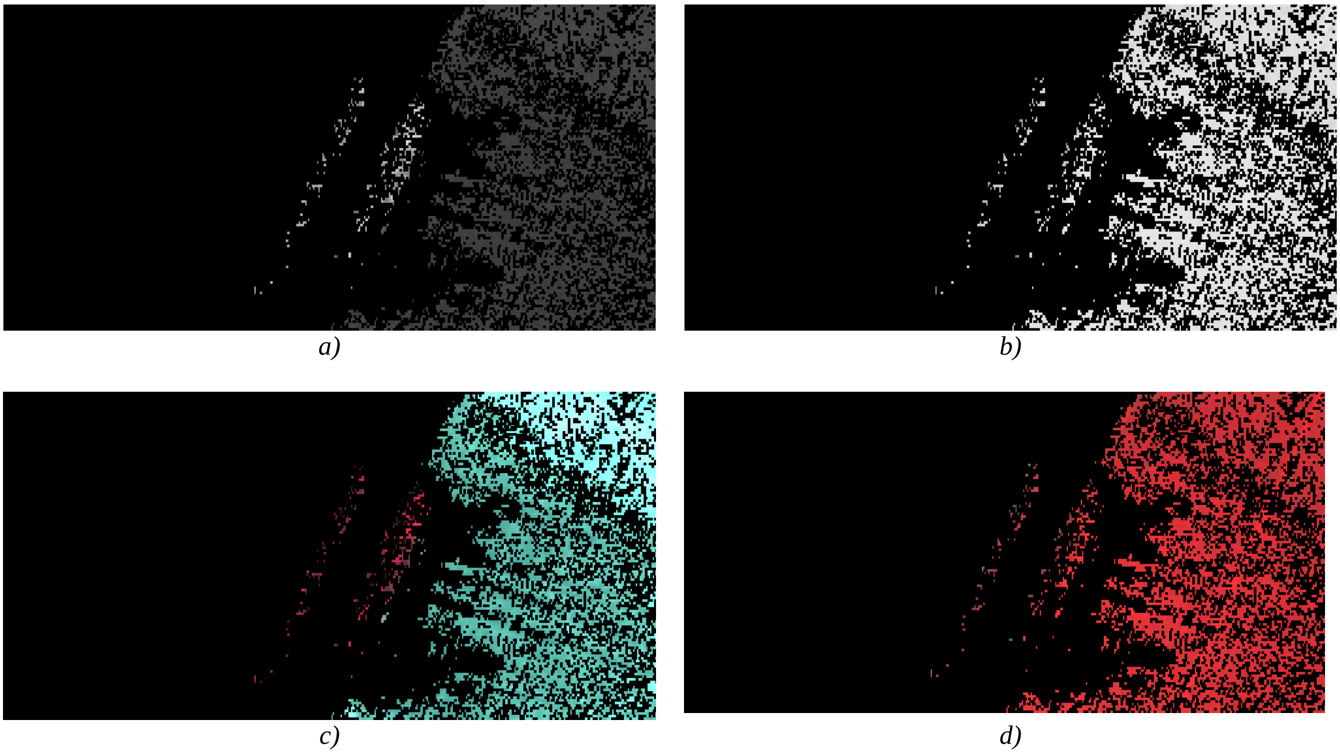

Figure 7. NDVI calculation results for multispectral segments of RG-changes, (7a, 7b) index gray-scale segments of the images obtained from QuickBird, May 15, 2007 and July 16, 2007, (7c, 7d) pseudocolor index images

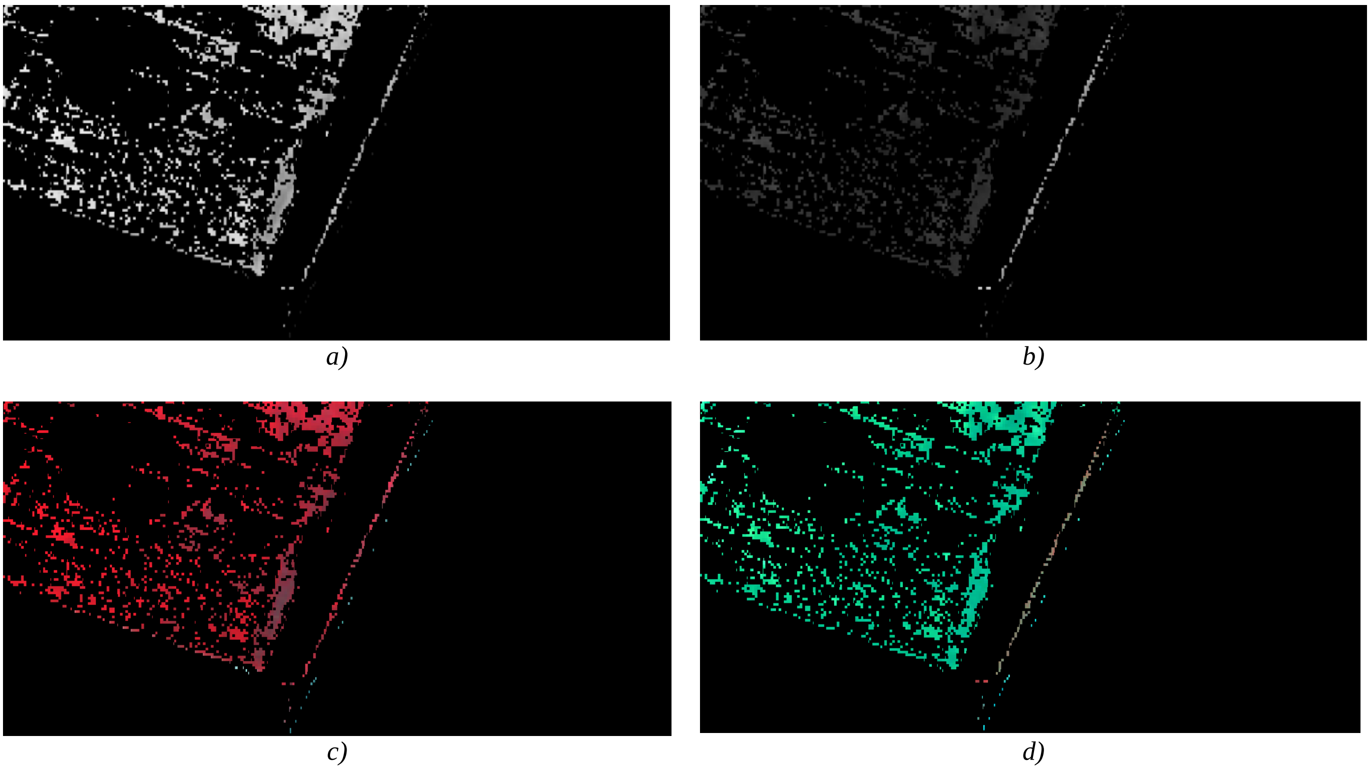

Figure 8. NDVI calculation results for multispectral segments of RB-changes, (8a, 8b) index gray-scale segments of the images obtained from QuickBird, May 15, 2007 and July 16, 2007, (8c, 8d) pseudocolor index images

For the calculated NDVI mean values and parts of the images, obtained from different satellites and used as the source images for the selected subareas of components of the objects' changes, see the table.

Table. NDVI mean value calculation for multispectral segments of changes

Spectra of changes	NDVI (Part of the image obtained from Landsat7 ETM+)			
	June 5		July 27	
RG	-0.177285	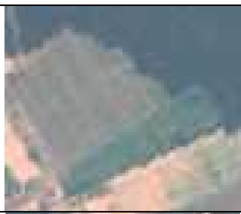	0.048167	
RGB	0.156553		0.123759	
	NDVI (Part of the image obtained from QuickBird)			
	May 15		July 16	
RG	-0.012029	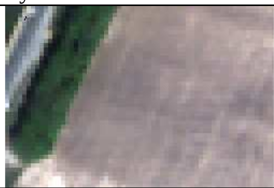	0.64909416	
RB	0.549692		0.041571	

This table demonstrates the trends of the vegetation condition on the particular component of the Earth surface area that was selected automatically and analyzed using the appropriate software. Different colors are used to depict the areas with different phytomass volumes. For the vegetation, the index is positive; the higher is the phytomass growth level, the higher these indices are. The calculated values of the vegetation index for the images obtained from the Landsat satellite demonstrate that there is no dynamics of the vegetation in the observed components of the object during the summer. However, it can be seen from Figures 5 and 6 that the degrees of uniformity of the multispectral segments of changes are different. This is because of the limited spatial resolution of the satellite imagery data for this area; as a result, during the selective brightness-based segmentation at the first stage of the procedure, the non-uniform areas of the monitored object were included in the selected interval, affecting the calculation of the vegetation index mean value. Figures 7 and 8 demonstrate both growth of the vegetation within the selected RG segment (see Figure 7) and its reduction during two summer months, maybe as a result of harvesting (see Figure 8). Due to high spatial resolution of the imagery, the components of the monitored Earth surface area, uniform in terms of texture, were clearly selected.

5. Conclusion

Because no vegetation indices can provide absolute quantitative characteristic of the property that is subject to investigation, and these indices' values depend on the sensor characteristics (spectral channel width, resolution), survey conditions, illumination and atmospheric conditions [3], the calculated NDVI for each subarea of the component of changes in the object's space was a contribution to the automatic evaluation of the vegetation condition in general. The developed algorithms provide automatic classification of changes caused by vegetation within the calendar periods for which the satellite survey data are available. As a result, these changes can be subdivided into multispectral sets of segments of the Earth surface area that is subject to observation, and their relation with the space-time variability can be determined by way of the brightness-based ranges of segments, developed and implementable as software, in the changes of the multispectral image.

To ensure that the proposed algorithms are implemented correctly, the existing ground observation data, the results of visual interpretations of the satellite imagery and the expert knowledge are necessary.

6. References

[1] Savin I.Yu., Lupyan E.A., Bartalev S.A.: Operating satellite monitoring of the agricultural crops condition in Russia. Geomatics, 2011, № 2, p. 69-76.

[2] Devyatova N.V., Ershov D.V.: MODIS/TERRA imagery in the monitoring of the insect pest outbreaks. Modern problems of the Earth remote sensing from the space. Vol. II. Moscow, 2005. p. 262-266.

[3] Cherepanov A.S., Druzhinina E.G.: Vegetation spectral properties and vegetation indices. Geomatics №3, 2009, p. 28-32.

[4] Lupyan E.A., Mazurov A.A., Nazirov R.R., Proshin A.A., Flitman E.V., Krasheninnikova Yu.S.: Technologies for the design of the information systems for the remote monitoring. Modern problems of the Earth remote sensing from the space, 2011, Vol. 8, №1, p.26-43.

[5] Belozerskii L. A., Oreshkina L.V.: Estimation of the Informative Content of Histograms of Satellite Images in the Recognition of Changes in Local Objects. Pattern Recognition and image Analysis, 2010, Vol. 20, No. 1, p. 65-72.

[6] Belozerskii L. A., Areshkina L.V.: Principles of the selective brightness-based segmentation of changes of appearance for the object of the monospectral satellite imagery. Artificial intelligence, 2009, №3, p. 395-408.
[7] Singh, A.: Digital change detection techniques using remotely-sensed data. International Journal of Remote Sensing, 1989, 10(6), p.989-1003.
[8] Lu D., Mausel P. et al.: Change detection techniques. Int. J. Rem. Sens., 2004, Vol. 25, №12, p. 2365-2407.
[9] Belozerskyy L.A., Areshkina L.V.: Histograms of satellite images and status of objects / Belozerskyy L.A., Areshkina L.V.: International Conference on Neural Networks and Artificial Intelligence ICNNAI'2008. May 27-30, 2008, Minsk, Belarus, p. 193-197.
[10] Richard J., Radke S.A., Omar, A.K., Badrinath, R.: Image Change Detection Algorithms: A Systematic Survey, IEEE Transactions on Image Processing, 2005, 14(3), p.294-307.
[11] Areshkina L.V.: Using the different-time satellite imagery for detection of changes of appearance of the monitoring objects / Areshkina L.V.: Proc. of the International scientific and technical conference. Donetsk: Nauka i Osvita Institute: 2010. p. 331-335.
[12] Vygotskaya N.N., Gorshkova L.I.: Theory and experiment in the remote vegetation researches. Gidrometeoizdat Publ., Leningrad, 1987, p. 249.
[13] Legend for NDVI images [Electronic data]. Mode of access: http://kaluga.infospace.ru/kaluga/html/legend.html - Date of access: July 30, 2011.